Journal of The Electrochemical Society, **159** (7) D431-D436 (2012)
0013-4651/2012/159(7)/D431/6/$28.00 © The Electrochemical Society

Preparation of Highly Uniform and Monodisperse PS/Cu Composite Microspheres Using Electroless Plating

Yuehui Ma and Qinghua Zhang[z]

State Key Laboratory for Modification of Chemical Fibers and Polymer Materials, College of Materials Science and Engineering, Donghua University, Shanghai 201620, China

Highly uniform and monodisperse core-shell microspheres composed of a polystyrene (PS) core and a copper shell were prepared by dispersion polymerization of styrene followed by electroless copper plating. The formation of copper shell on PS surface was confirmed by FESEM, TEM, XRD and TGA. As a result, the plating bath composition had an important influence on the morphology of PS/Cu composites. The addition of Na_2EDTA and La_2O_3 as a complexant and a stabilizer led to the formation of a more compact copper shell on PS surface. The formation mechanism was explored by the linear sweep voltammetry method, and the different morphology might mostly result from the various nucleation rates. Tailoring of shell thickness can be achieved through altering the loading of PS in the ECP bath. Conductivity of the PS/Cu composites with a shell thickness of 195 nm is up to 2.2×10^5 S/m. The PS/Cu composites may have great potential to be used as fillers of anisotropic conductive film for their uniform diameter, low density and good conductivity.
© 2012 The Electrochemical Society. [DOI: 10.1149/2.045207jes] All rights reserved.

Manuscript submitted February 28, 2012; revised manuscript received March 27, 2012. Published July 17, 2012.

As the requirements for interconnection and joining materials in microelectronics packaging applications have moved toward ultra-fine-pitch bonding and environmental friendliness, anisotropic conductive film (ACF) has gained much attention as an alternative to tin/lead (Sn/Pb) solders.[1,2] ACF not only allow products to be thinner, smaller and lighter, but also offer good electrical performance and stability.[3]

ACFs mainly consist of polymeric binder matrices and conductive fillers.[4] When heat and pressure are applied during bonding, the electric connection is established only in the Z-direction by using a relatively low weight loading of conductive fillers, typically 1–10 wt%.[5] Originally, carbon fibers were used as the conductive fillers for ACF. Then, the fillers were replaced by lead-free solder spheres and metal spheres, such as nickel, silver and gold-coated Ni spheres.[6] For instance, there has been growing interest in copper with various sizes and shapes used as filler of isotropic or anisotropic conductive adhesive owing to its high electrical, thermal conductivity, low cost and electro-migration tendency.[7–10]

However, the high density and cost of metal spheres are not beneficial to the filler of ACF. Recently, polyaniline coated polystyrene-divinylbenzene microspheres for potential application in ACF were reported by Wang et al.[11] But the relative low bulk (6.67×10^{-3} S/cm) conductivity of PSDVB/PANi limited its application in ACF. Therefore, based on the consideration of maintaining high reliability and reducing the cost, the polymer/metal composite microspheres have been widely added into an insulating adhesive matrix to prepare ACF in recent years.[12] Polystyrene (PS) is often selected as the polymeric core on account of the similar coefficient of thermal expansion (CTE) between PS and thermosetting adhesive matrix in the ACF. In other words, the ACF composed of adhesive matrix and PS/metal microspheres can bring about an improvement in thermal stability.[13] In addition, the elastic deformation of PS under the thermal compression results in a larger contact area between two electrodes. For metal layer of composite microspheres, Au[14–16] and Au coated Ni[17–19] are always used in interconnection with high requirement for their good chemical stability and excellent conductivity. However, their high cost is one of the drawbacks for wide use in interconnection.

Previous reports on the preparation methods of core-shell structure have shown that electroless plating is one of the most effective techniques to form uniform coating on all surfaces, regardless of size, shape and electrical conductivity.[20–23] But it still remains difficult to be used in the formation of metal layer onto the polymer microspheres surface owing to the existence of hoop stresses.[14] In particular, the composite microspheres used for ACF should be strong enough to sustain blending and thermal bonding.[12,15] Therefore, the preparation of monodisperse PS/Cu composite microspheres with uniform, complete and stable shells by electroless plating is still a key challenge.

Development of a new filler with high conductivity and low density for ACF is the goal of this work. To the best of our knowledge, few report is related to the preparation of Cu coated PS microspheres used for the filler in ACF up to now. Here, electroless plating technology was selected to prepare such Cu coated PS microspheres filler. The catalytic sites (palladium seeds) are introduced onto the PS surface by activating treatment to initiate electroless copper plating (ECP) process. The morphology and electrical properties of the PS/Cu composites were investigated.

Experimental

Materials.— Styrene (St) was purchased from Shanghai Chemical Reagent Co. (China) and purified by treatment with 5 wt% aqueous NaOH solution to remove the inhibitor. Poly (vinylpyrrolidone) (PVP, M_w = 30000), 2,2-azobisisobutyroitrile (AIBN), absolute ethanol, concentrated sulfuric acid, hydrochloric acid (37%), tin (II) chloride dehydrate, palladium (II) chloride, copper sulfate, ethylenediaminetetraacetic acid disodium salt (Na_2EDTA), potassium sodium tartrate (PST), triethanolamine (TEA), formaldehyde (HCHO), 2,2-dipyridyl and lanthanum oxide were all purchased from Shanghai Chemical Reagent Co. (China) and used as received. Deionized water was used for rinsing and preparation of all solutions.

Synthesis of PS microspheres.— The monodisperse PS microspheres were prepared by dispersion polymerization.[24] St (5 g), PVP (0.5 g) and AIBN (0.05 g) were dissolved in ethanol (30 g). The reaction mixture was heated at 70°C and the polymerization was conducted under an N_2 atmosphere for 24 h. The product was repeatedly rinsed with ethanol in order to remove the remaining PVP and St. Then PS microspheres were dried at 60°C in vacuum for further use.

Synthesis of PS/Cu composite microspheres.— Electroless plating was carried out by multi-step processes, including roughing, sensitization, activation and electroless plating. The pretreatment of PS microspheres were carried out using a previously reported procedure.[25] The activated PS microspheres were then rinsed with deionized water and dried at 60°C in vacuum for further use. The ECP solution is composed of main salt ($CuSO_4 \cdot 5H_2O$ 0.06 M), reductant (HCHO 12 mL/L), complexing agent (Na_2EDTA, $C_4H_4O_6KNa\cdot4H_2O$ or TEA), pH adjustant (NaOH) and additive (2,2-dipyridyl or La_2O_3). The pH value of the standard ECP bath is 12. The activated PS microspheres were then immersed into the ECP solution for 15 min at 30°C. Finally, the samples were rinsed with deionized water and dried in vacuum at 60°C.

[z]E-mail: qhzhang@dhu.edu.cn

Downloaded on 2016-09-11 to IP 130.203.136.75 address. Redistribution subject to ECS terms of use (see ecsdl.org/site/terms_use) unless CC License in place (see abstract).

All the experiments were accomplished under ultrasonication, including the pretreatment of PS microspheres and the preparation of PS/Cu composite microspheres.

Characterization.— The morphology of samples was observed by field emission scanning electron microscopy (FESEM, Hitachi S-4800), scanning electron microscopy (SEM, Hitachi TM-1000) and transmission electron microscope (TEM, JEOL JEM-1010). Energy dispersive X-ray (EDX, Oxford IE 300X) analysis of Pd decorated PS was performed on an EDAX system attached to SEM (JEOL, JSM-5600LV). X-ray diffraction (XRD, Rigaku D-max-2500) measurements were conducted on a diffractometer with nickel-filtered Cu K_α radiation $\lambda = 0.154$ nm. Thermogravimetric analysis (TGA, NETZSCH TG209F1) of the composite microspheres was performed in a nitrogen atmosphere at a heating rate of 20°C/min. An inductively coupled plasma mass spectroscopy (ICP-MS, Prodigy, Leeman Labs) was used to detect the levels of La. The density of the samples at 25°C was determined by means of a nitrogen pycnometer (Quantachrome Ultrapycnometer 1000). The density was measured for at least three times to obtain an average value. The electrical property of each sample was measured with a four-point probe system (MCP-T360, Mitsubishi Chemical). PS/Cu composites were compressed into sheets by tablet press machine to reduce the influence from the contact resistance.

For linear sweep voltammetry (LCV), a 3 cm^2 copper sheet, a commercial electrode of Ag/AgCl saturated with KCl and a platinum wire were used as the working sheet, reference and counter electrodes, respectively. LSV experiments were carried out at 25°C and at a scan rate of 20 mV/s. The anodic polarization curves were measured in the bath without copper ion and the cathodic polarization curves were measured in the same composition bath without formaldehyde.

Results and Discussion

Figure 1 shows the typical SEM image of monodisperse pristine PS microspheres with smooth surface and uniform size. It is well known that PS is an insulating substrate. Therefore, one of the most important factors dominating Cu shell layer deposition is the activation of PS microspheres prior to ECP process.[26] As the color changes from white to brown, the decoration of PS microspheres by Pd seeds is accomplished. Figure 2 shows the typical energy-dispersive X-ray analysis (EDX) of the sample after a two-step process treated using $SnCl_2$ and $PdCl_2$ solutions. It can be found that there are some small peaks of Pd besides the peak of carbon. These metallic Pd seeds provide the catalytic activity which is required for the subsequent deposition of copper on PS surface.

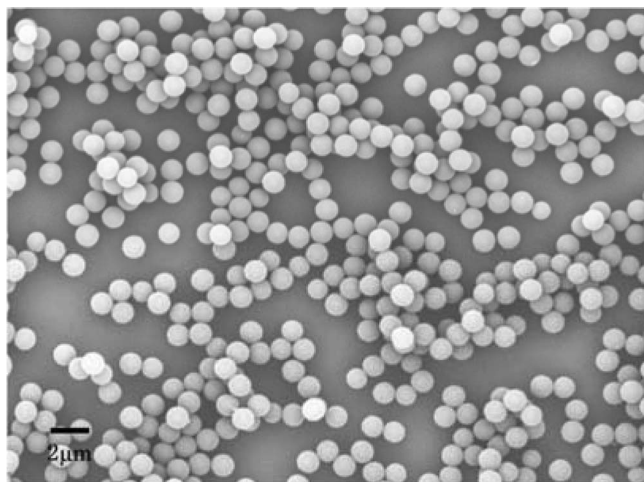

Figure 1. SEM images of pristine PS prepared by dispersion polymerization.

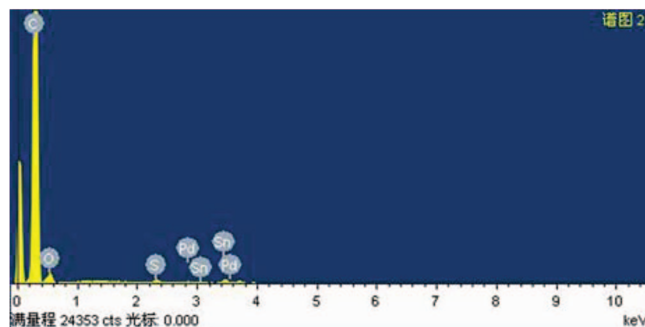

Figure 2. EDX patterns of palladium decorated PS microspheres.

Generally, ECP progress differs from normal chemical reduction of cupric ions in a water solution where cupric ions are produced everywhere.[27] The deposition of copper is formed only on the surface which is decorated by catalyst sites. As is well known, formaldehyde is widely used as a reductant for ECP owing to the high catalyst activity of Cu for the anodic oxidation of formaldehyde.[28,29] According to the studies of Ohno et al.,[29,30] formaldehyde is substantially the only reductant which can be used in high speed ECP process. The increase of coverage of Cu on substrate results in an increased deposition rate. Though numerous studies on the mechanism of ECP have been carried out, no definitive mechanism has been established.[31,32] In generally, it is now widely accepted that ECP process is a redox reaction occurred at the interface between the substrate and plating solution. On the basis of the mixed potential theory, electroless plating proceeds along the lines of an electrochemical mechanism as the simultaneous reaction of cathodic metal deposition and anodic oxidation of reductant.[30,33] The overall reaction can be expressed as:[34]

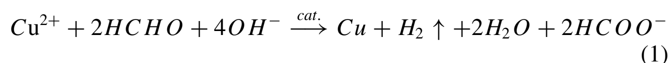

$$Cu^{2+} + 2HCHO + 4OH^- \xrightarrow{cat.} Cu + H_2 \uparrow + 2H_2O + 2HCOO^- \quad (1)$$

According to previous studies, the reducing ability of formaldehyde is dependent on the pH value of plating bath and concentration of formaldehyde.[20,35] Lin et al.[36] reported the effect of concentration of formaldehyde on the reducing ability using linear sweep voltammetric method. They found that the anodic peak current density increased upon increasing the concentration of formaldehyde, but the increase was limited by the total number of available active sites. We have also obtained a similar result, which is shown in Figure 3a. We chose 12 mL/L as the concentration of formaldehyde in this paper. Figure 3b shows the LSV curves for formaldehyde oxidation in 0.08 M Na_2EDTA solution at various pH adjusted by NaOH. The peak at -0.4 V – -0.3 V is assigned to the anodic oxidation peak of formaldehyde. It can be found that the pH of plating bath should be above 10 for formaldehyde to be used as a reductant. These results are in good agreement with those of Xu[20] and Lim.[35] The reducing ability of formaldehyde increases obviously with the increase of pH of plating bath, and the proper pH for our ECP process is determined to be 12.

In our study, the mode of feeding formaldehyde has an influence on the morphology of PS/Cu composites to some extent, which is shown in Figure 4. When activated PS microspheres are added into the ECP bath containing copper-complex and formaldehyde, an unsatisfactory result is obtained. As shown in Figure 4a, the situation of peel-off of the plating layer from the polymeric matrix and aggregation of metal-plated polymeric particles occurs. However, when formaldehyde is dripped in the dispersion of PS microspheres and copper-complex solution under ultrasonication, the monodisperse PS/Cu composite microspheres are prepared with continuous shell (Figure 4b). The difference in the morphology of PS/Cu composites prepared by two modes may be a result of different deposition rates which are resulted from the redispersion of Pd decorated PS microspheres into ECP bath. In addition, formaldehyde must be previously adsorbed on the surface of activated PS microspheres before the oxidation of formaldehyde

Downloaded on 2016-09-11 to IP 130.203.136.75 address. Redistribution subject to ECS terms of use (see ecsdl.org/site/terms_use) unless CC License in place (see abstract).

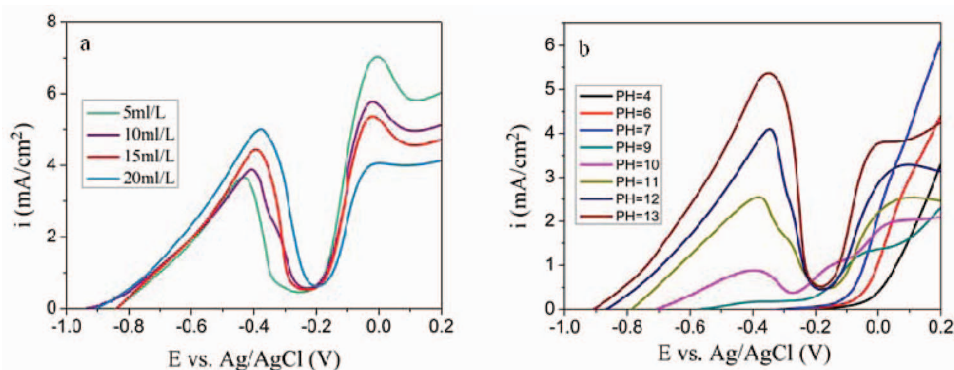

Figure 3. Effects of the concentration of HCHO (a) and pH (b) on the anodic polarization behaviors.

proceeds.[36] When formaldehyde is added dropwise, a relatively uniform adsorption results in the formation of regular PS/Cu composites.

Owing to the high pH of ECP bath, complexing agents are added into the plating bath to prevent the formation of $Cu(OH)_2$. Three kinds of complexing systems are adopted herein to prepare PS/Cu composites based on a series of previous studies.[20,21,36] As can be seen from Figure 5a and 5c, monodisperse PS/Cu composite microspheres with uniform and complete shell are obtained when Na_2EDTA or a dual-complexing system of Na_2EDTA-PST are used as a chelating agent, respectively; whereas, an incomplete copper shell is produced when the dual-complexing system of Na_2EDTA-TEA is used as the chelating agent. On the other hand, some free Cu particles around the PS core can be observed, as highlighted using a circle in Figure 5b.

To explore the influences of complexing systems on the morphology of PS/Cu composite microspheres, LSV measurements are used to investigate the polarization behaviors in various conditions, which are shown in Figure 5d. It is known that the chelating capability of Na_2EDTA to copper (II) ions is much stronger than that of PST or TEA. Therefore, there is a slight difference in the cathodic polarization behavior among these complexing systems, since most copper (II) ions are chelated by Na_2EDTA. On the other hand, there exists an obvious difference in the anodic polarization behavior, as shown in Figure 5d. For anodic scans, an additional oxidation peak around 0 V can be assigned to the stripping peak of Cu electrode.[37] The decreased oxidation current intensity around 0V indicates that the dual-complexing system of Na_2EDTA-PST effectively suppresses the oxidation of Cu electrode. The huge steric hindrance of Cu(II)-EDTA and Cu(II)-PST near the electrode surface may be a reason for this result. In contrast, the presence of TEA not only decreases the formaldehyde oxidation peak current intensity but also promotes the dissolution of Cu electrode. In Na_2EDTA-TEA dual-complexing system, the main effect of TEA is the adsorption on substrates under the condition of sufficient Na_2EDTA.[36] The adsorption will inhibit the oxidation of formaldehyde to a certain extent, as the –OH terminal groups of TEA can react with formaldehyde to form acetals.[31] On the other hand, the initiation rate of ECP process is very low, since palladium exhibits a relative low active for the anodic oxidation of formaldehyde.[30] All above illustrations may contribute to explain the formation of incomplete copper shell with Na_2EDTA-TEA as chelating agent, as shown in Figure 5b.

It is well-known that the copper-plating bath is unstable owing to the relatively high reduction potential of cupric ions [$E_{25^\circ C}{}^0$(NHE) = 0.340 V].[38] One way to compensate for the poor stability of ECP process is to add stabilizer into the plating solution.[39] Figure 6a is a typical FESEM image of PS/Cu composite microspheres prepared without stabilizer, exhibiting a continuous and rough shell. In previous studies, 2,2-dipyridyl has been widely used as additive to form coating on the flat surface with improved microstructure and physical properties.[33,40,41] Thus, 50 ppm 2,2-dipyridyl is added into the ECP bath. However, cubic copper particles with a three-dimension are produced on PS surface, as shown in Figure 6b. To further improve the shell morphology, 50 ppm La_2O_3 as a stabilizer is added into the ECP bath. Interestingly, a dense and smooth shell with smaller grains is produced, as shown in Figure 6c. ICP-MS measurement shows that La is co-deposited on PS surface with copper, accounting for about 0.085 wt% of shell.

The XRD patterns of PS/Cu composites prepared with various plating bath are shown in Figure 6d. The peaks at 2θ angles of 43.4, 50.6, 74.3 and 90.1 correspond to the reflections of (111), (200), (220) and (311) crystalline planes of the face center cubic (fcc) structure of Cu, respectively. All diffraction peaks match well with these of fcc Cu crystal (JCPDS No. 65-9743)[42] and no impurity diffraction peaks were detected, revealing that high pure metallic copper exists within the shell layer. As shown in Figure 6d, the addition of La_2O_3 in the plating bath enhances diffraction peak intensities of the composites, which demonstrates an increasing crystallinity of copper shell.

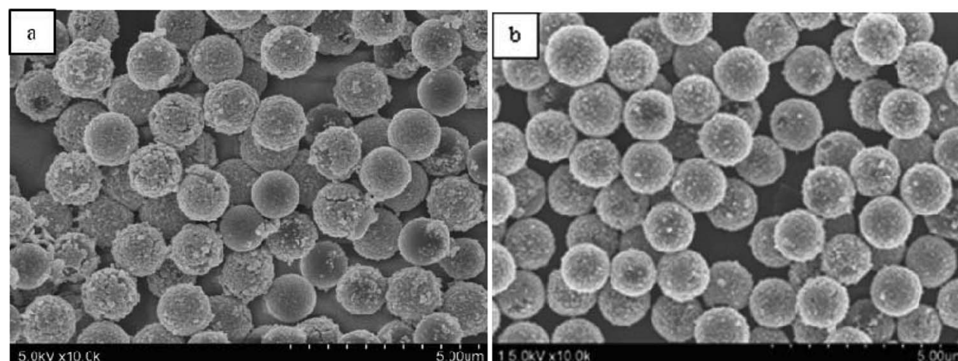

Figure 4. FESEM images of PS/Cu composites prepared by various feeding modes of HCHO: (a) PS was added in the mixture of copper-complex solution and HCHO; (b) HCHO was dripped in the dispersion of PS and copper-complex solution.

Downloaded on 2016-09-11 to IP 130.203.136.75 address. Redistribution subject to ECS terms of use (see ecsdl.org/site/terms_use) unless CC License in place (see abstract).

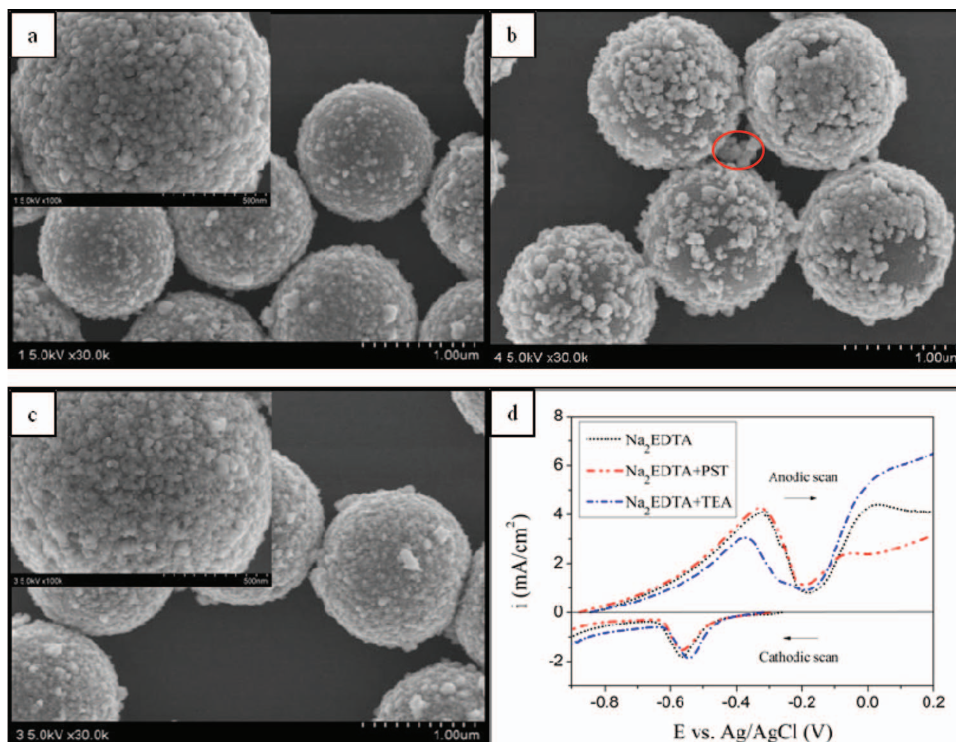

Figure 5. FESEM images (a–c) of PS/Cu composites prepared with various complexing systems and their corresponding polarization behaviors (d). (a) 0.08 M Na_2EDTA; (b) 0.08 M Na_2EDTA+ 0.06 M TEA; (c) 0.08 M Na_2EDTA + 0.06 M PST.

Bulk conductivity of PS/Cu composites are inserted in Figure 6d. Apparently, the similar values of three kinds of PS/Cu composites derived from various plating bath suggest that the additives has a slight influence on the conductivity.

Based on the mixed potential theory, the anodic and cathodic current must be equal at a common potential (known as mixed potential), and the current density (known as mixed current density) at such potential can be used to predict the deposition rate of ECP.[43,44] Using

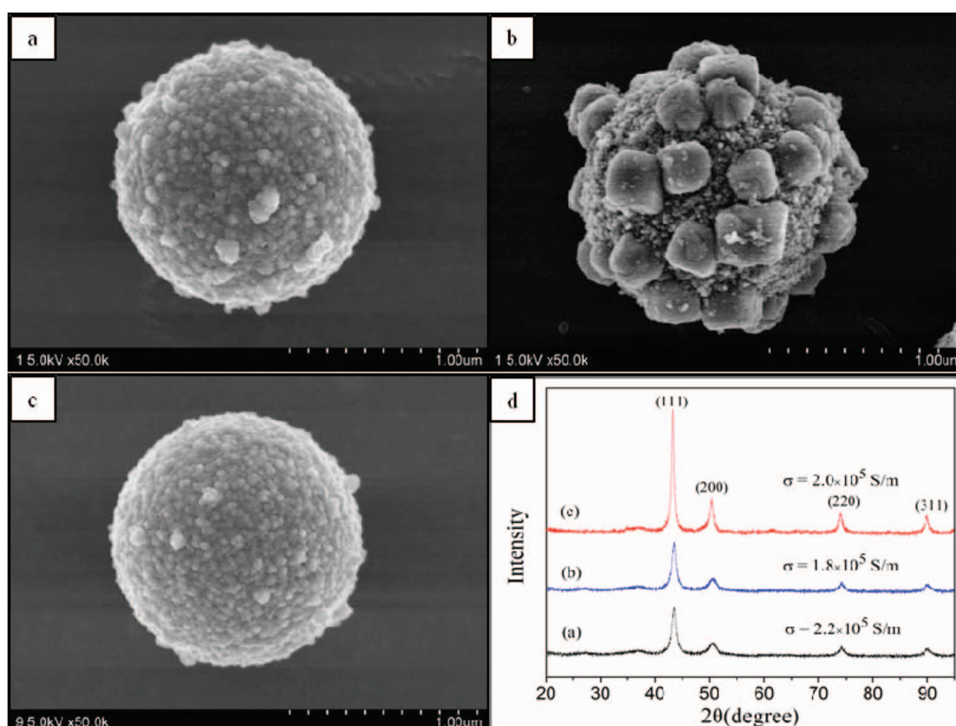

Figure 6. FESEM images (a–c) and XRD patterns (d) of PS/Cu composites prepared with various additives in ECP bath: (a) no additive; (b) 2,2-dipyridyl (c) La_2O_3.

Downloaded on 2016-09-11 to IP 130.203.136.75 address. Redistribution subject to ECS terms of use (see ecsdl.org/site/terms_use) unless CC License in place (see abstract).

Faraday's law, the rate of copper deposition can be estimated as:

$$v_{(\mathrm{mg\ cm^{-2}h^{-1}})} = \frac{\Delta W}{St} = \frac{M}{n}\cdot\frac{Q}{F}\cdot\frac{1}{St} = \frac{M}{n}\cdot\frac{i}{F} = 1.19 i_{(\mathrm{mA\ cm^{-2}})} \quad (2)$$

Where, ΔW (mg) is the mass of the reacting substances on electrode, S (cm^2) is the surface area of the electrode, M (kg mol^{-1}) is the mole mass of the reacting substances, n is the chemical measure coefficient of electrode reaction, F is the Faraday constant (26.8 A h), i (mA cm^{-2})is the mixed current density, *and* v (mg cm^{-2} h^{-1}) is the deposition rate.

Figure 7 shows the anodic and cathodic polarization curves with and without additives in the plating solution. It can be seen clearly that the addition of 2,2-dipyridyl causes a decrease in the magnitude of the oxidation peak current density, which leads to a negative shift of the mixed potential from −0.593 V to −0.611 V and a decrease of mixed current from 1.18 mA cm^{-2} to 0.88 mA cm^{-2} for electroless copper deposition. In other words, compared to the additive-free plating bath, the deposition rate of ECP is reduced from 1.40 mg cm^{-2} h^{-1} to 1.05 mg cm^{-2} h^{-1} due to the presence of 2,2-dipyridyl. Unlike 2,2-dipyridyl, when La_2O_3 was added, the oxidation peak potential of formaldehyde shifts to the negative direction and reduction peak current density of cupric complex ions increases, which causes a increase of mixed current to 2.105 mA cm^{-2} and thus accelerates the deposition rate of copper (2.50 mg cm^{-2} h^{-1}).

Lin et al. reported the crystallization process of Cu film during the ECP process systematically.[45–47] They suggested that the nucleus was prone to grow as a large grain of micrometer order in a lower nucleation rate system. 2,2-Dipyridyl would adsorb on the surface of activated PS microspheres when it is added into the plating bath. The adsorption causes a lower rate of electron transfer or nucleation.[33] Therefore, during the deposition process of copper in the presence of 2,2-dipyridyl, the growth of nuclei might become predominant. Cu nanoparticles with a smaller size form firstly, and then grow to form a bigger one, as shown in Figure 6b. However, the special electronic structure endows lanthanum with much amount of nuclear charge, very intensive adsorptive capacity and surface activity.[48] So the adsorption of La^{3+} on PS surface might offer an amount of electronic orbit holes or free electrons, leading to a decrease in surface energy and an increase in nucleation rate.[49] The coalescence of uniform nanocrystallites forms upon repeated 3D nucleation at a higher nucleation rate. In addition, it has been proved that rare earth element can reduce surface tension and interfacial energy between the generated H_2 bubble and the as-deposited layer.[50] It might be anticipated that the porous structure resulted from the emission of hydrogen during HCHO oxidation process disappears, causing a smoother and denser copper layer, as shown in Figure 6c.

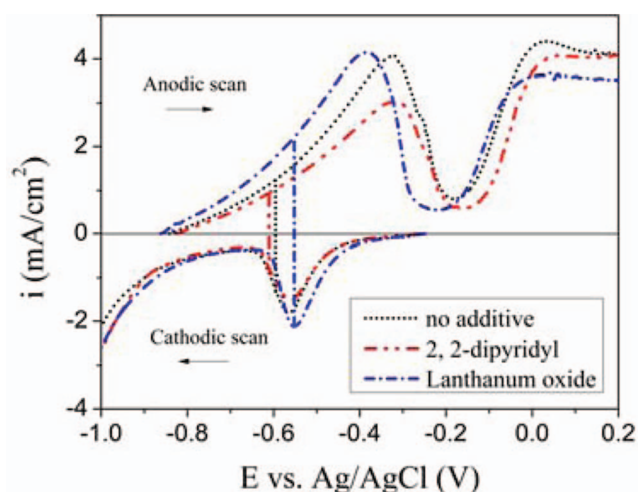

Figure 7. Polarization behaviors of ECP bath (mixed potential) under various conditions.

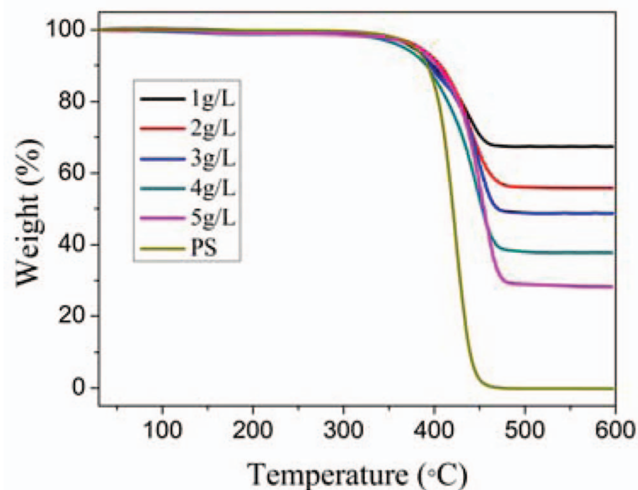

Figure 8. TGA of PS and PS/Cu composites prepared with various loading of PS.

During the process of ECP, the thickness of copper shell can be easily tuned by altering the loading of PS. The loading herein is defined as the weight of activated PS introduced to 1 L ECP solution.[51] Figure 8 shows the TGA curves of the original PS and PS/Cu composites prepared with various loading of PS. As can be seen, PS completely decomposes at the temperature above 500°C, which is caused by the pyrolysis of polystyrene to H_2, CH_4, and other gases,[52] so the residual weight should be the weight of copper shell. According to the TGA curves, the shell contents of samples prepared with various loading of PS (1-5 g/L) are evaluated to be 67.3%, 55.8%, 48.6%, 37.8% and 28.2%. Meanwhile, the initial thermo-decomposing temperature of PS/Cu composites obviously increased, indicating that the continuous shell layer has formed on PS microspheres as well.[53] The thickness of copper shell correspond to various loading of PS is listed in Table I. An increase in shell thickness of PS/Cu composites is observed when the loading of PS decreased under the same reaction conditions. Additionally, the densities of PS/Cu composites prepared with various loading are listed in Table I. The values of PS/Cu composites increase gradually from 1.568 g/cm^3 to 2.821 g/cm^3 with the loading of PS decreasing from 5 g/L to 1 g/L, which is significantly lower than the density of pure Cu powder of 8.92 g/cm^3. The smaller density gap between the filler and the polymer matrix (ca. 1 g/cm^3) will overcome the sedimentation problem, which frequently occurs in the blend of high-density metal fillers with the low density polymer matrices.[54] Furthermore, the electrical properties of Cu-coated PS microspheres were also investigated in order to apply to an ACF, which are listed in Table I. As anticipated, with the increase of loading of PS in the ECP bath, the bulk conductivity of resulting PS/Cu composites apparently increases. In summary, tailoring of the shell thickness, density and conductivity of the PS/Cu composites can be achieved through variation in the loading of PS.

Table I. Shell thickness and density of each PS/Cu composites with various weight ratio of Cu to PS.

Loading (g/L)	Shell thickness (nm)	Density of composites (g/cm^3)	Conductivity (S/m)
5	58	1.568	0.3×10^0
4	90	1.691	1.9×10^1
3	135	1.993	9.8×10^2
2	162	2.312	8.1×10^4
1	195	2.821	2.2×10^5

Downloaded on 2016-09-11 to IP 130.203.136.75 address. Redistribution subject to ECS terms of use (see ecsdl.org/site/terms_use) unless CC License in place (see abstract).

Conclusions

High quality continuous Cu shell with high conductivity was obtained by direct electroless plating on PS microspheres. Palladium seeds decorated on PS surface served as nucleation sites to initiate ECP process. The monodisperse PS/Cu composite microspheres with continuous shell can be obtained with Na_2EDTA or Na_2EDTA-PST as complexing system when formaldehyde was dripped in the dispersion of PS and copper-complex solution. However, in the Na_2EDTA-TEA system, an incomplete copper shell formed on PS surface. The addition of 2,2-dipyridyl or La_2O_3 as a stabilizer had a different influence on the deposition rate of copper by electrochemical measurements, and thus led to a various morphology of PS/Cu composite microspheres. As the mechanism discussed above, the different morphology resulted from the various nucleation rates. In addition, the thickness of copper shell, density and conductivity of PS/Cu composites can be easily tuned by altering the loading of PS. The density of composites increased from 1.568 g/cm^3 to 2.821 g/cm^3 when the loading of PS changed from 5 g/L to 1g/L, and the bulk conductivity of PS/Cu composites increased from 0.3 S/m to 2.2×10^5 S/m, corresponding to the shell thickness of 58 nm to 195 nm. Therefore, the monodisperse PS/Cu composite microspheres with low density and good conductivity may have great advantages in the fields of ACF. This method is suitable for the mass production and it is expected to play a significant role in the development of ACF.

Acknowledgments

Financial support of this work is provided by NSFC (51173024, 50873021), SRFDP (20110075110009), Shuguang Plan (09SG30), Shanghai Leading Academic Discipline Project (B603), and the 111 Project (111-2-04).

References

1. Y. Li, K. S. Moon, and C. P. Wong, *Science*, **308**, 1419 (2005).
2. Y. C. Lin and J. Zhong, *J. Mater. Sci.*, **43**, 3072 (2008).
3. J. Kyung-Woon and P. Kyung-Wook, *IEEE T. Compon. Pack. T.*, **32**, 339 (2009).
4. Y. Li and C. P. Wong, *Mat. Sci. Eng. R*, **51**, 1 (2006).
5. M. J. Yim, Y. Li, K. S. Moon, and C. P. Wong, *J Electron. Packaging*, **132**, 011007 (2010).
6. M. Yim, Y. Li, K. Moon, and C. P. Wong, *J. Electron. Mater.*, **36**, 1341 (2007).
7. Z. Rongwei, L. Wei, M. Kyoung-Sik, L. Qizhen, and C. P. Wong, *IEEE T. Compon. Pack. T.*, **1**, 25 (2011).
8. Y. S. Lin and S. S. Chiu, *J. Adhes. Sci. Technol.*, **22**, 1673 (2008).
9. K. L. Chan, M. Mariatti, Z. Lockman, and L. C. Sim, *J. Mater. Sci.: Mater. Electron.*, **21**, 772 (2010).
10. H. Zhao, T. Liang, and B. Liu, *Int. J. Adhes. Adhes.*, **27**, 429 (2007).
11. L. Wang, J. Xu, Y. Chen, S. Cheng, and L. J. Fan, *J. Polym. Res.*, **18**, 2169 (2011).
12. J. Ma, H. Gao, and X. Chen, *Adv. Mater. Res.*, **194**, 643 (2011).
13. S. I. Asai, U. Saruta, M. Tobita, M. Takano, and Y. Miyashita, *J. Appl. Polym. Sci.*, **56**, 769 (1995).
14. Y. Yamamoto, S. Takeda, H. Shiigi, and T. Nagaoka, *J. Electrochem. Soc.*, **154**, D462 (2007).
15. S. Tokonami, Y. Yamamoto, Y. Mizutani, I. Ota, H. Shiigi, and T. Nagaoka, *J. Electrochem. Soc.*, **156**, D558 (2009).
16. J. H. Lee, D. O. Kim, G. S. Song, Y. Lee, S. B. Jung, and J. D. Nam, *Macromol. Rapid Comm.*, **28**, 634 (2007).
17. J. H. Lee, Y. Lee, and J. D. Nam, *Intermetallics*, **17**, 365 (2009).
18. J. H. Lee, J. S. Oh, P. C. Lee, D. O. Kim, Y. Lee, and J. D. Nam, *J. Electron. Mater.*, **37**, 1648 (2008).
19. J. H. Lee, Y. Lee, and J. D. Nam, *Surf. Interface Anal.*, **42**, 36 (2010).
20. C. Xu, G. Wu, Z. Liu, D. Wu, T. T. Meek, and Q. Han, *Mater. Res. Bull*, **39**, 1499 (2004).
21. S. L. Zhu, L. Tang, Z. D. Cui, Q. Wei, and X. J. Yang, *Surf. Coat. Tech.*, **205**, 2985 (2011).
22. G. Ling and Y. Li, *Mater. Lett.*, **59**, 1610 (2005).
23. D. Gao and M. Zhan, *Appl. Surf. Sci.*, **255**, 4185 (2009).
24. C. M. Tseng, Y. Y. Lu, M. S. El-Aasser, and J. W. Vanderhoff, *J. Polym. Sci. Pol. Chem.*, **24**, 2995 (1986).
25. Y. Ma, Q. Zhang, and Y. Li, *J. Electrochem. Soc.*, **159**, D119 (2012).
26. I. Lee, P. T. Hammond, and M. F. Rubner, *Chem. Mater.*, **15**, 4583 (2003).
27. X. Yin, L. Hong, and B. H. Chen, *J. Phys. Chem. B*, **108**, 10919 (2004).
28. J. Li and P. A. Kohl, *J. Electrochem. Soc.*, **150**, C558 (2003).
29. I. Ohno, O. Wakabayashi, and S. Haruyama, *J. Electrochem. Soc.*, **132**, 2323 (1985).
30. O. Izumi, *Mat. Sci. Eng. A*, **146**, 33 (1991).
31. P. Lu and A. V. Walker, *Langmuir*, **23**, 12577 (2007).
32. D. Plana, A. I. Campbell, S. N. Patole, G. Shul, and R. A. W. Dryfe, *Langmuir*, **26**, 10334 (2010).
33. J. Li, *Electrochim. Acta*, **49**, 1789 (2004).
34. C. A. Deckert, Electroless copper plating. A review. I. *Plat. Surf. Finish.*, **82**, 48 (1995).
35. V. W. L. Lim, E. T. Kang, and K. G. Neoh, *Synthetic Met.*, **123**, 107 (2001).
36. Y. M. Lin and S. C. Yen, *Appl. Surf. Sci.*, **178**, 116 (2001).
37. Y. J. Zheng, F. X. Xiao, W. H. Zou, and Y. Wang, *J. Cent. South. Univ. T.*, **15**, 669 (2008).
38. C. H. Chen, B. H. Chen, and L. Hong, *Chem. Mater.*, **18**, 2959 (2006).
39. F. Hanna, Z. A. Hamid, and A. A. Aal, *Mater. Lett.*, **58**, 104 (2004).
40. M. Oita, M. Matsuoka, and C. Iwakura, *Electrochim. Acta*, **42**, 1435 (1997).
41. R. S. Liu, C. C. You, M. S. Tsai, S. F. Hu, Y. H. Li, and C. P. Lu, *Solid State Commun.*, **125**, 445 (2003).
42. M. Joo, B. Lee, S. Jeong, and M. Lee, *Appl. Surf. Sci.*, **258**, 521 (2011).
43. J. Li and P. A. Kohl, *J. Electrochem. Soc.*, **149**, C631 (2002).
44. X. Wang, N. Li, Z. Yang, and Z. Wang, *J. Electrochem. Soc.*, **157**, D500 (2010).
45. H. H. Hsu, J. W. Yeh, and S. J. Lin, *J. Electrochem. Soc.*, **150**, C813 (2003).
46. C. H. Lai, Y. C. Sung, S. J. Lin, S. Y. Chang, and J. W. Yeh, *Electrochem. Solid ST.*, **8**, C114 (2005).
47. H. H. Hsu, C. W. Teng, S. J. Lin, and J. W. Yeh, *J. Electrochem. Soc.*, **149**, C143 (2002).
48. T. Xuan, L. Zhang, and S. Feng, *J. Rare Earth.*, **24**, 393 (2006).
49. J. Li, Y. Tian, Y. Li, and X. Wang, *J. Rare Earth.*, **28**, 769 (2010).
50. D. Liu, L. Zhou, J. Yu, Y. Yan, and K. Lee, *Mater. Corros.*, **62**, 926 (2011).
51. W. Zhao, Q. Zhang, H. Zhang, and J. Zhang, *J. Alloy. Compd.*, **473**, 206 (2009).
52. N. Kawahashi and H. Shiho, *J. Mater. Chem.*, **10**, 2294 (2000).
53. W. Wang, Y. Jiang, S. Wen, L. Liu, and L. Zhang, *J. Colloid Interf. Sci.*, **368**, 241 (2011).
54. A. Ho, J. Chang, W. K. Chin, and H. T. Hsieh, *J. Polym. Res.*, **13**, 285 (2006).

Downloaded on 2016-09-11 to IP 130.203.136.75 address. Redistribution subject to ECS terms of use (see ecsdl.org/site/terms_use) unless CC License in place (see abstract).